

Supporting Information

A facile wet chemistry approach towards unilamellar tin sulfide nanosheets from $\text{Li}_{4x}\text{Sn}_{1-x}\text{S}_2$ solid solutions

Alexander Kuhn,^a Tanja Holzmann,^a Viola Doppel,^a Jürgen Nuss,^a and Bettina V. Lotsch^{a,b*}

- a) Max Planck Institute for Solid State Research, Heisenbergstr. 1, 70569 Stuttgart, Germany.
b) Department of Chemistry, Ludwig-Maximilians-Universität München, Butenandtstr. 5-13, 81377 München, and Nanosystems Initiative Munich (NIM) & Center for Nanoscience, Schellingstr. 4, 80799 München, Germany

1. Structural details

Table S1. Crystallographic details of Li_2SnS_3 as obtained from single-crystal X-ray diffraction using Mo- K_α radiation.

Li_2SnS_3	slowly cooled down	melt-quenched
temperature	298 K	298 K
space group (number)	$C2/c$ (15)	$R\bar{3}m$ (166)
lattice constants	$a = 6.3961(7)$ Å $b = 11.0893(13)$ Å $c = 12.4157(14)$ Å $\beta = 99.860(2)^\circ$	$a = 3.6868(2)$ Å $a = 3.6868(2)$ Å $c = 18.300(2)$ Å $\gamma = 120^\circ$
cell volume	$V = 867.62(17)$ Å ³	$V = 215.42(3)$ Å ³
unit cell content	$Z = 8$	$Z = 2$
radiation	Mo K_α	Mo K_α

max 2Θ	69.42°	69.20°
index range	$-9 \leq h \leq 10$	$-5 \leq h \leq 5$
	$-17 \leq k \leq 17$	$-5 \leq k \leq 5$
	$-19 \leq l \leq 19$	$-28 \leq l \leq 28$
total reflections	6216	1091
unique reflections	1754	143
R_{int}	0.028	0.027
R_1	0.054	0.021
$wR2$	0.162	0.055
$GooF$	1.54	1.48
deposition number	CSD-426848	CSD-426849

Table S2. Atomic coordinates for monoclinic Li_2SnS_3 (space group $C2/c$) and rhombohedral Li_2SnS_3 (space group $R\bar{3}m$) as obtained from single-crystal X-ray diffraction using Mo- $K\alpha$ radiation.

Li_2SnS_3 average structure in $R\bar{3}m$						
site	Wyck.	x	y	z	occ.	$U_{\text{eq}} (\text{\AA}^2)$
SnLi	$3b$	0	0	1/2	Sn 2/3 Li 1/3	0.00487(19)
Li	$3a$	0	0	0	1	0.0148(25)
S	$6c$	0	0	0.24653(5)	1	0.00867(33)
Li_2SnS_3 superstructure in $C2/c$						
site	Wyck.	x	y	z	occ.	$U_{\text{eq}} (\text{\AA}^2)$
SnLi1	$4e$	0	0.74977(5)	1/4	Sn 0.966(4) Li 0.034(4)	0.0127 (2)
SnLi2	$4e$	0	0.08315(5)	1/4	Sn 0.953(4) Li 0.047(4)	0.0132(3)
SnLi3	$4e$	0	0.4151(6)	1/4	Sn 0.080(6) Li 0.920(6)	0.023(2)

Li1	8f	0.248(2)	0.0840(13)	-0.0002(12)	1	0.028(3)
Li2	4d	1/4	1/4	1/2	1	0.030(5)
S1	8f	0.11268(26)	0.08521(13)	0.63106(14)	1	0.0147(4)
S2	8f	0.13487(24)	0.24069(13)	0.13088(13)	1	0.0136(4)
S3	8f	0.36583(26)	0.08948(15)	0.37062(14)	1	0.0162(4)

Details of the Rietveld refinement for the 2D freestanding film:

The Rietveld refinement of the XRD pattern shown in Fig 7C was performed with the TOPAS software. Although this software is designed for 3D crystals, we used a quasi 2D model to simulate the structure of the 2D crystals. Therefore, we first analyzed the symmetry of the 2D crystal structure which is constructed of edge-sharing octahedra. Such a layer of equal octahedra has the plane group $p3m1$. For the refinement with TOPAS, the space group $P\bar{3}m1$ (no. 164) was used, which results in stacking of identical 2D layers in an eclipsed fashion along the c -axis, such that the 2D projection of the 3D structure along c is identical to that of a single layer. In order to simulate a quasi 2D structure, we chose an arbitrary but very large value for the separation of the S-Sn-S layers along the c -axis (here: 330 Å). Using a very large cell still results in discrete reflections in reciprocal space instead of continuous rods as expected for a true 2D crystal, but already a small broadening of the discrete reflections applied to the model leads to the continuous behavior as expected for a true 2D crystal, which would be obtained as a limit when the layer separation reaches infinity.

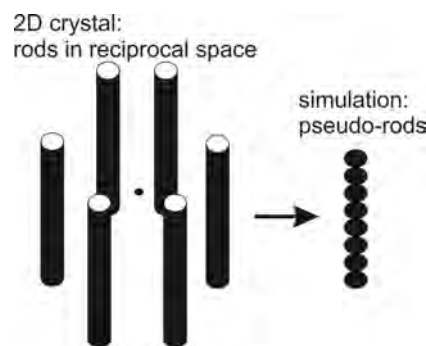


Figure S1. Schematic picture of the representation a 2D crystal in reciprocal space and its simulation with a 3D periodic structure of layers separated by large distances.

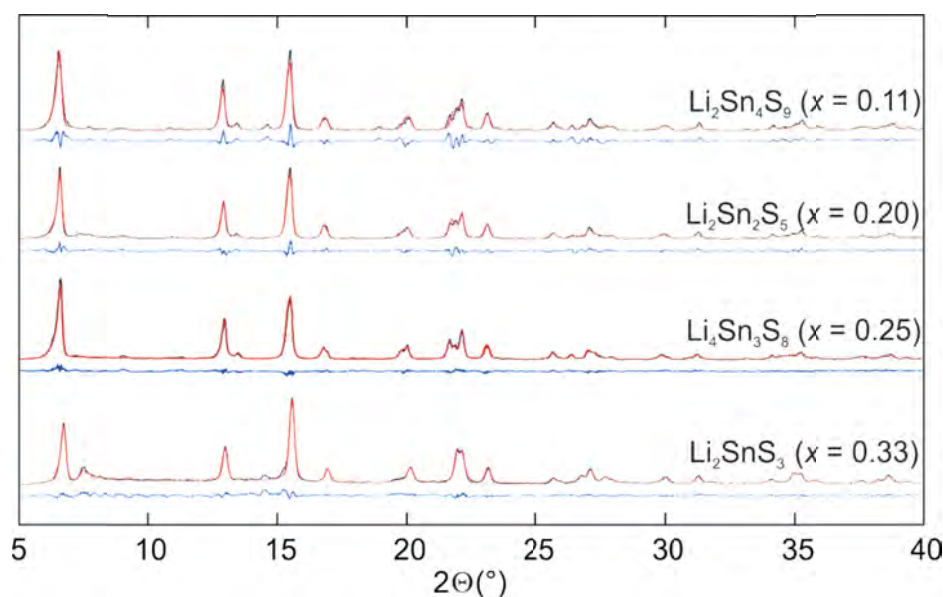


Figure S2. Rietveld refinements of $\text{Li}_{4x}\text{Sn}_{1-x}\text{S}_2$ with $0.11 \leq x \leq 0.33$ (black dots), refined based on the monoclinic crystal structure of Li_2SnS_3 as obtained from single crystal diffraction. Hereby, the occupancies of the SnLi positions (see Table S2) were refined and were equal to the expected values within 5%.

2. Chemical composition

Table S3. SEM-EDX data of Li_2SnS_3 (in at-%).

Spectrum	S	Sn
Spectrum 1	74.60	25.40
Spectrum 2	72.53	27.47
Spectrum 3	74.70	25.30
Spectrum 4	73.10	26.90
Mean	73.73	26.27
Std. deviation	1.08	1.08
Max.	74.70	27.47
Min.	72.53	25.30

Table S4. SEM-EDX data of Li₄Sn₃S₈ (in at-%).

Spectrum	S	Sn
Spectrum 1	72.35	27.65
Spectrum 2	71.31	28.69
Spectrum 3	71.81	28.19
Mean	71.82	28.18
Std. deviation	0.52	0.52
Max.	72.35	28.69
Min.	71.31	27.65

Table S5. SEM-EDX data of Li₂Sn₂S₅ (in at-%).

Spectrum	S	Sn
Spectrum 1	70.83	29.17
Spectrum 2	70.35	29.65
Spectrum 3	70.86	29.14
Spectrum 4	70.43	29.57
Spectrum 5	70.73	29.27
Spectrum 6	71.34	28.66
Mean	70.76	29.24
Std. deviation	0.35	0.35
Max.	71.34	29.65
Min.	70.35	28.66

Table S6. SEM-EDX data of $\text{Li}_2\text{Sn}_4\text{S}_9$ (in at-%).

Spectrum	S	Sn
Spectrum 1	70.11	29.89
Spectrum 2	69.68	30.32
Spectrum 3	66.87	33.13
Spectrum 4	69.27	30.73
Mean	68.98	31.02
Std. deviation	1.45	1.45
Max.	70.11	33.13
Min.	66.87	29.89

Table S7. SEM-EDX data of the nanosheet pellet after centrifugation at 15000 rpm and drying at 110 °C (in at-%).

Spectrum	S	Sn
Spectrum 1	64.65	35.35
Spectrum 2	65.93	34.07
Spectrum 3	65.31	34.69
Mean	65.30	34.70
Std.	0.64	0.64
deviation		
Max.	65.93	35.35
Min.	64.65	34.07

Table S8. SEM-EDX data of the nanosheet pellet after rotary evaporation of the solvent at 70 °C (in at-%).

Spectrum	S	Sn
Spectrum 1	71.93	28.07
Spectrum 2	68.80	31.20
Spectrum 3	70.21	29.79
Mean	70.31	29.69
Std. deviation	1.57	1.57
Max.	71.93	31.20
Min.	68.80	28.07

Table S9. ICP-AES results of nanosheet (NS) pellet after centrifugation, NS suspension, supernatant after centrifugation, and bulk material.

Material	Li [wt-%]	Sn [wt-%]	Atomic ratio Li : Sn
NS pellet of $\text{Li}_2\text{Sn}_2\text{S}_5$ after centrifugation (measurement 1)	1.7	47.89	1.00 : 1.64
NS pellet of $\text{Li}_2\text{Sn}_2\text{S}_5$ after centrifugation (measurement 2)	1.69	47.75	1.00 : 1.69
NS pellet of $\text{Li}_2\text{Sn}_2\text{S}_5$ after 3 washing steps and centrifugation (measurement 1)	0.7	65.17	1.00 : 5.44
NS Suspension of $\text{Li}_2\text{Sn}_2\text{S}_5$	29.44	510.14	1.00 : 1.01

Supernatant of NS suspension after centrifugation at 15000 rpm for 30 minutes	15.06	53.44	4.82 : 1.00
Bulk of $\text{Li}_2\text{Sn}_2\text{S}_5$	3.25	56.09	1.00 : 1.00
NS pellet of $\text{Li}_2\text{Sn}_2\text{S}_5$ after annealing at 450 °C (measurement 1)	1.04	63.69	1.00 : 3.58
NS pellet of $\text{Li}_2\text{Sn}_2\text{S}_5$ after annealing at 450 °C (measurement 2)	1.05	65.43	1 : 3.65

3. AFM images

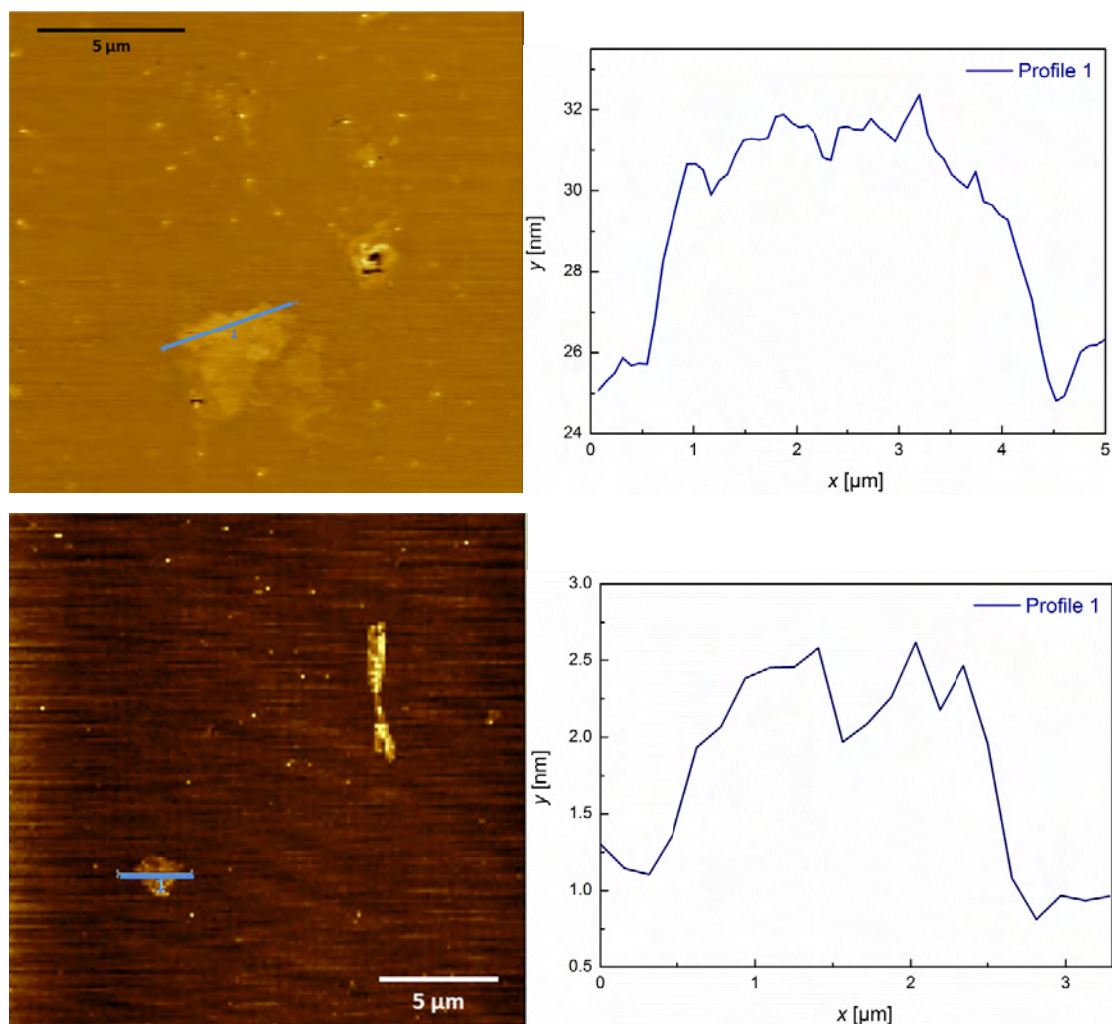


Figure S3. Left: AFM images of nanosheets from a $\text{Li}_2\text{SnS}_3/\text{H}_2\text{O}$ nanosheet suspension deposited on a Si/SiO₂(300nm) wafer. Right: Respective height profiles. Height: 4 nm (top), 1.5 nm (bottom).

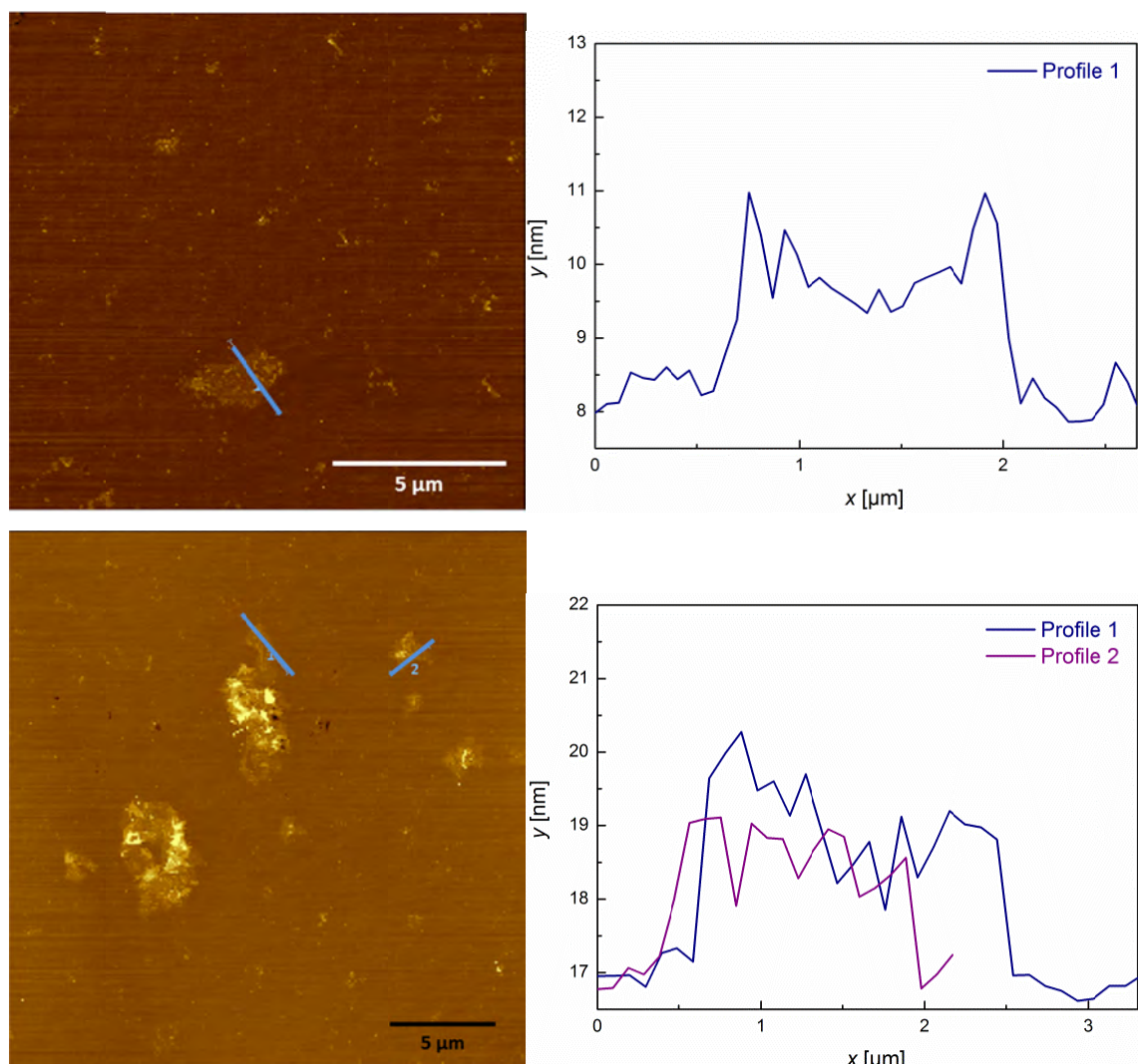


Figure S4. Left: AFM images of nanosheets from a $\text{Li}_4\text{Sn}_3\text{S}_8/\text{H}_2\text{O}$ nanosheet suspension deposited on a Si/SiO₂(300nm) wafer. Right: Respective height profiles. Height of the nanosheets: approx. 2 nm.

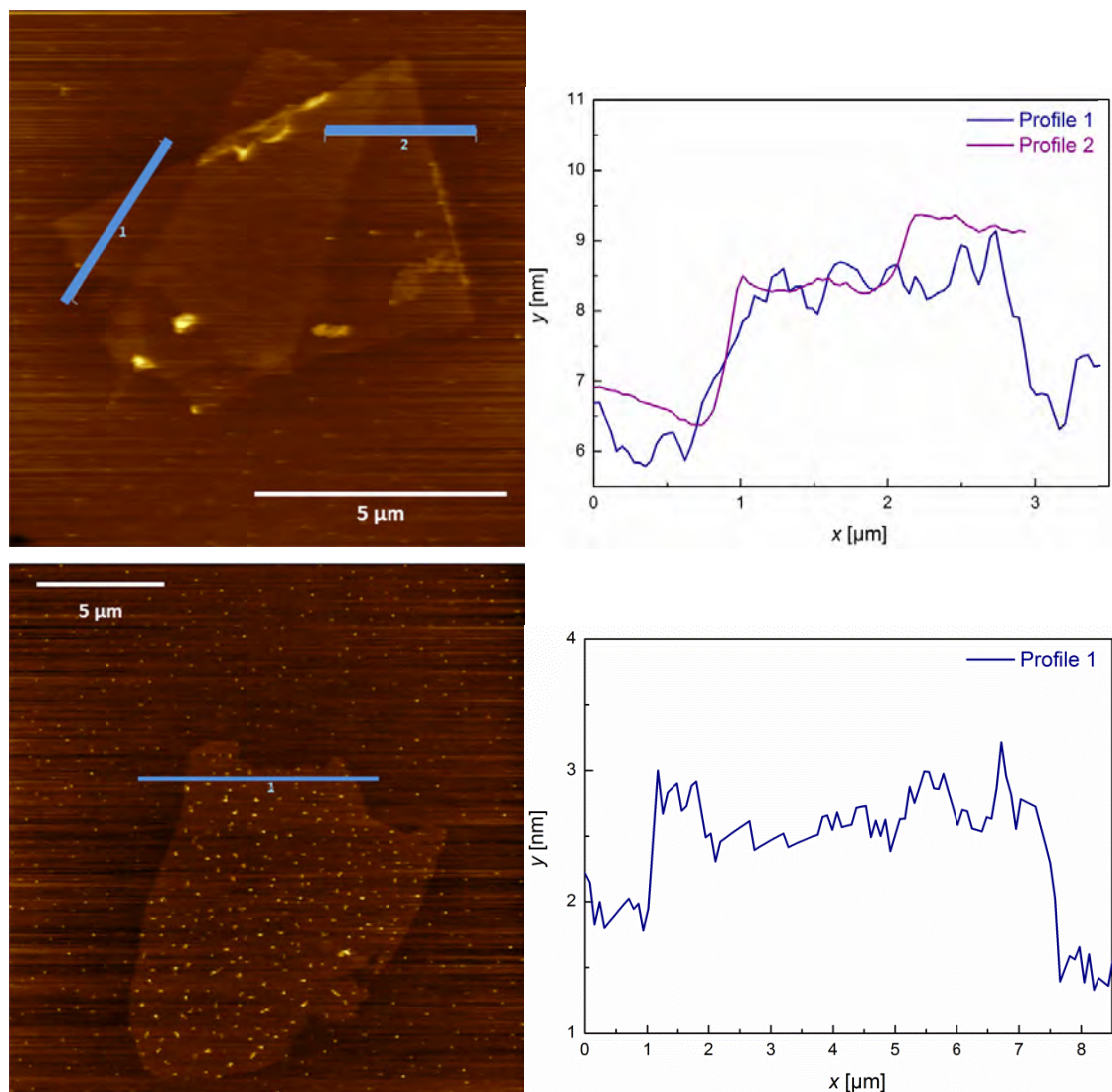


Figure S5. Left: AFM images of nanosheets from a $\text{Li}_2\text{Sn}_2\text{S}_5/\text{H}_2\text{O}$ nanosheet suspension deposited on a $\text{Si}/\text{SiO}_2(300\text{nm})$ wafer. Right: Height profile of two overlapping single sheets (top, about 1 nm height) and height profile of a single nanosheet, showing a height of 1 nm (bottom).

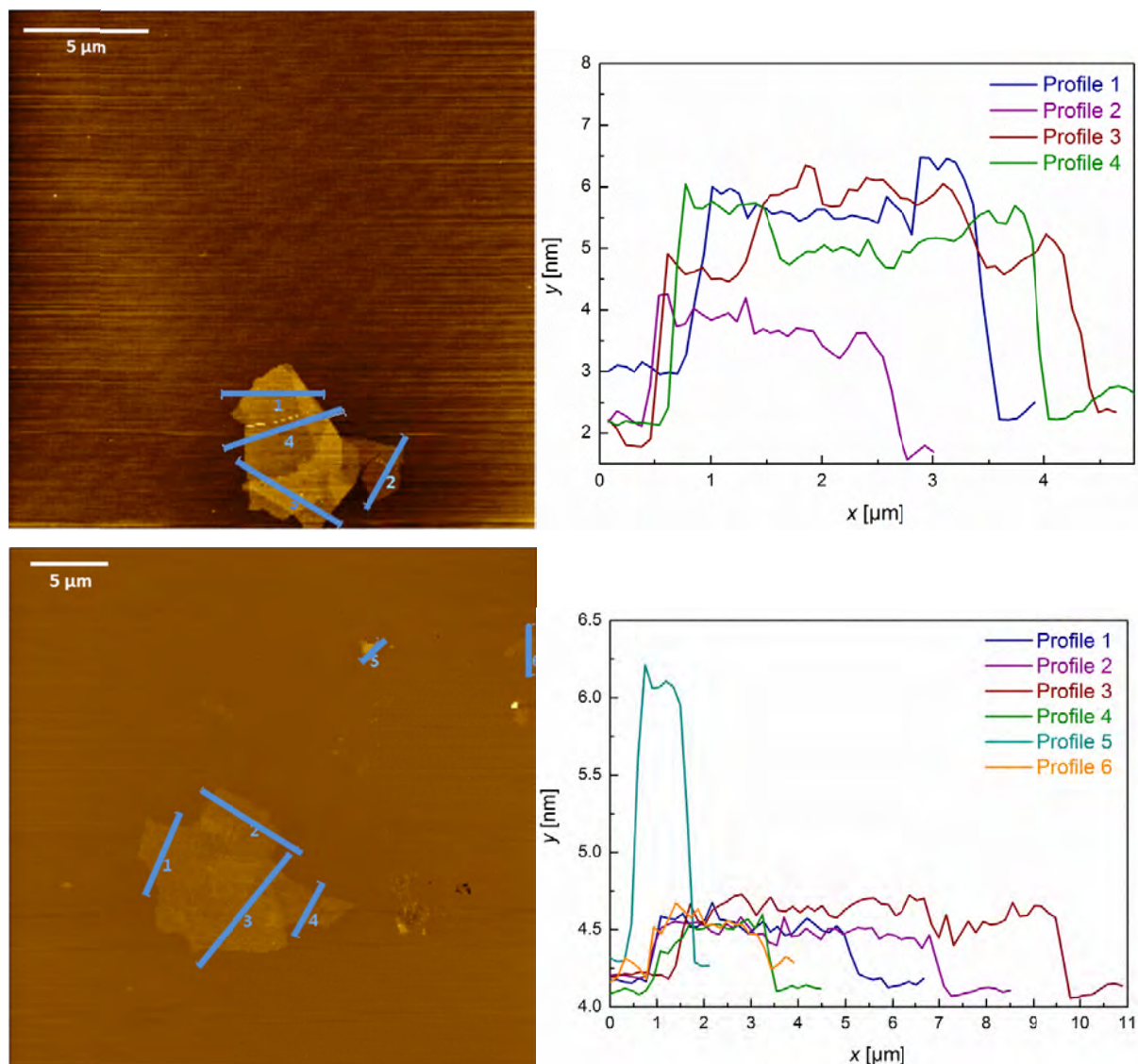


Figure S6. Left: AFM images of nanosheets from a $\text{Li}_2\text{Sn}_4\text{S}_9/\text{H}_2\text{O}$ nanosheet suspension deposited on a $\text{Si}/\text{SiO}_2(300\text{nm})$ wafer. Right: Top: folded and stacked sheets with individual height of 2 and 1 nm. Bottom: large nanosheet with a height of 0.6 nm.

4. TEM images

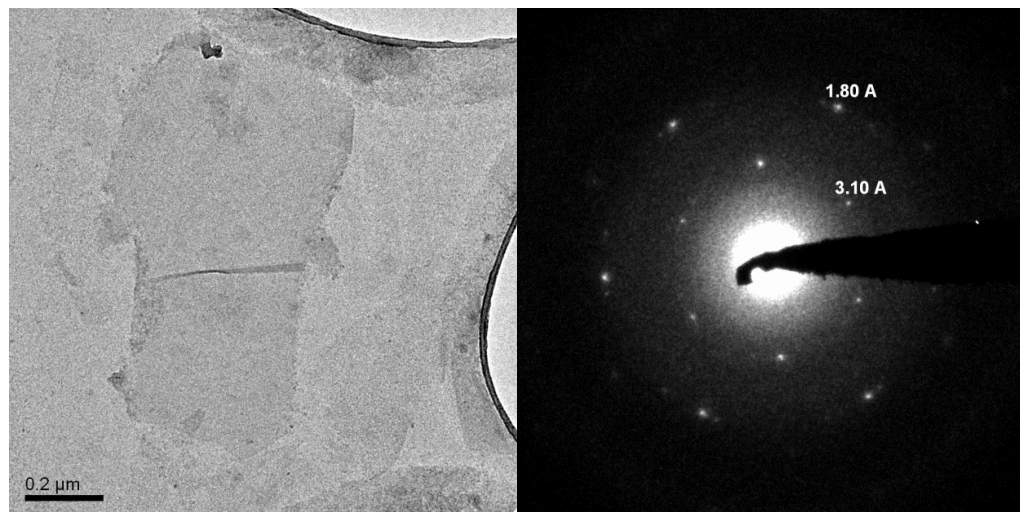


Figure S7. Left: TEM image of a nanosheet obtained by drop-casting a $\text{Li}_2\text{SnS}_3/\text{H}_2\text{O}$ nanosheet suspension on a lacey carbon film/copper grid. Right: SAED pattern of the nanosheet shown on the left.

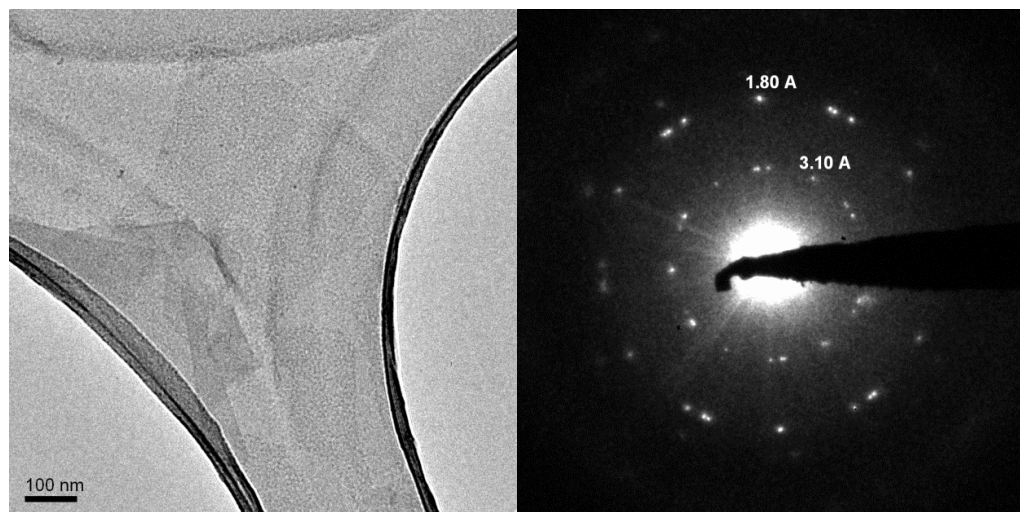


Figure S8. Left: TEM image of a nanosheet obtained by drop-casting the $\text{Li}_4\text{Sn}_3\text{S}_8/\text{H}_2\text{O}$ nanosheet suspension on a lacey carbon film/copper grid. Right: SAED pattern of the nanosheet shown on the left.

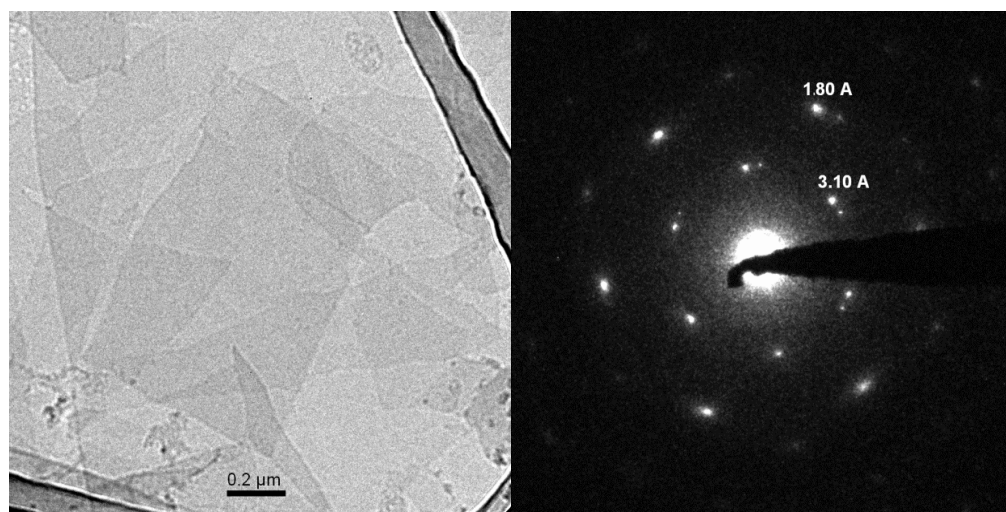


Figure S9. Left: TEM image of a nanosheet obtained by drop-casting the $\text{Li}_2\text{Sn}_4\text{S}_9/\text{H}_2\text{O}$ nanosheet suspension on a lacey carbon film/copper grid. Right: representative SAED pattern of the nanosheet shown on the left.

5. Kubelka-Munk spectrum

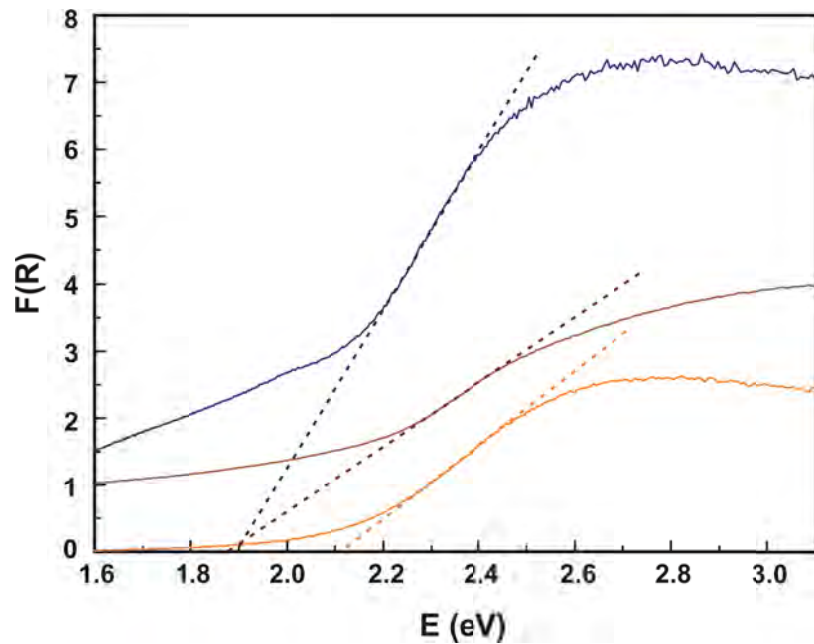


Figure S10. Kubelka-Munk spectra of bulk $\text{Li}_2\text{Sn}_2\text{S}_5$ (blue line), the nanosheet film (pellet) after centrifugation and drying (yellow line) and the annealed nanosheet pellet (brown line). The straight lines indicate the linear region of the absorption edges. Their cut with the x-axis gives the optical bandgap of the material, which is ≈ 1.9 eV for the bulk material $\text{Li}_2\text{Sn}_2\text{S}_5$ and the annealed nanosheet pellet, and ≈ 2.1 eV for the nanosheet pellet. Due to the smooth rather than ideally sharp absorption edges, these values should only be considered as a rough estimate.